

Endothelial deletion of adipose triglyceride lipase protects against heart failure with preserved ejection fraction

To the Editor: Heart failure with preserved ejection fraction (HFpEF) pathophysiology is multifactorial, with alterations in cardiac lipid metabolism likely playing a central role (1). Cardiac lipid metabolism is governed by transcellular uptake and transport of circulating lipids across cardiac endothelial cells (EC). In HFpEF, however, the processes of endothelial lipid handling and their functional relevance for lipid handling in the myocardium are largely unknown. Lipid processing in ECs relies on the function of the lipid droplet-hydrolyzing (LD-hydrolyzing) enzyme adipose triglyceride lipase (ATGL), the deletion or pharmacological blockade of which results in the accumulation of LDs in ECs (2–5).

EC-specific Atgl-KO mice (ecAtglKO) and their Cre WT littermate controls (Atgl^{fl/fl}) (Figure 1A) were subjected to the 2-hit (high-fat diet [HFD]/L-NAME) HFpEF protocol (Figure 1, B and C) (6). Echocardiography after 15 weeks revealed a preserved left ventricular (LV) ejection fraction (EF) and LV hypertrophy in both genotypes (Figure 1D and Supplemental Figure 1, A–C; supplemental material available online with this article; <https://doi.org/10.1172/jci.insight.187145DS1>). Surprisingly, ecAtglKO mice were protected against HFD/L-NAME-mediated diastolic dysfunction (Figure 1, E–H) and exhibited improved global longitudinal strain (GLS) (Figure 1, I and J, and Supplemental Figure 1, D and E).

HFpEF was associated with enhanced LD formation in cardiomyocytes with few LDs detected in capillary ECs (Figure 1, K and L). Endothelial ATGL deletion led to enhanced LD formation in ECs and a reduced LD cardiomyocyte/EC ratio (Figure 1, K and L). LV triacylglycerol (TAG) accumulation significantly increased in Atgl^{fl/fl}-HFpEF mice but not in ecAtglKO-HFpEF mice (Figure 1M and Supplemental Figure 1F). Distinct differences in mitochondrial or sarcomeric structure were not detected between Atgl^{fl/fl}-HFpEF and ecAtglKO-HFpEF mice (data not shown).

We next performed single nuclei RNA-Seq from LV samples (Figure 1, N–Q, and Supplemental Figure 2, A and B). Comparison of Atgl^{fl/fl}-HFpEF and ecAtglKO-HFpEF mice revealed 264 genes significantly upregulated and 261 downregulated in cardiomyocytes as well as 475 upregulated and 165 downregulated genes in capillary ECs (Figure 1, O and Q). We could not detect any clear inflammatory response in EC subclusters (Supplemental Figure 2, C and D, and Supplemental Figure 3). In cardiomyocytes from ecAtglKO-HFpEF mice, genes involved in FA metabolism were significantly upregulated (Figure 1R). Dysregulation of the unfolded protein response (UPR) has been recently identified as a pathogenic driver of HFpEF connected to lipid metabolism (6). Similarly, we found a significant reduction of cardiomyocyte genes involved in the IRE1 α /XBP1 signaling pathway of the UPR in Atgl^{fl/fl}-HFpEF mice (Figure 1S, left), accompanied by a reduction of IRE1 α phosphorylation (Supplemental Figure 4A) (6). This reduction was notably absent in ecAtglKO-HFpEF mice, and genes involved in protein processing in the ER were upregulated (Figure 1, S [right] and T, and Supplemental Figure 4A). Finally, pharmacological inhibition of ATGL in ECs resulted in increased LD formation in ECs and reduced LD detection in cardiomyocytes, associated with increased expression of Hspa5/BiP in cardiomyocytes (Supplemental Figure 4, B–D). In conclusion, endothelial-specific deletion of ATGL improved diastolic function in HFpEF accompanied by changes of neutral lipid storage at the capillary EC–cardiomyocyte interface. Mechanistically, reduced LD accumulation in cardiomyocytes may reverse the suppression of the IRE1 α /XBP1 axis of the UPR (Figure 1U) (6). In addition to the effects observed at the capillary EC–cardiomyocyte interface, systemic metabolic effects may have contributed to the HFpEF improvement in ecAtglKO mice. Recent publications demonstrate that endothelial ATGL deletion promotes endothelial dysfunction, arterial hypertension, and atherosclerosis mediated by the suppression of the eNOS/NO pathway (2–5). The unique property of our model is that this pathway was continuously blocked by L-NAME, which likely prevented the detection of detrimental effects of LD formation on NO-dependent function and contributed to the phenotype observed in ecAtglKO-HFpEF mice. Finally, it is important to note that the 2-hit HFpEF model used here also has limitations and that an analysis of endothelial ATGL in other HFpEF models would be recommended.

Authorship note: JS and MS contributed equally to this work. AFL and UK contributed equally to this work.

Conflict of interest: The authors have declared that no conflict of interest exists.

Copyright: © 2025, Schwanbeck et al. This is an open access article published under the terms of the Creative Commons Attribution 4.0 International License.

Submitted: September 16, 2024

Accepted: January 16, 2025

Published: March 10, 2025

Reference information: *JCI Insight*. 2025;10(5):e187145. <https://doi.org/10.1172/jci.insight.187145>.

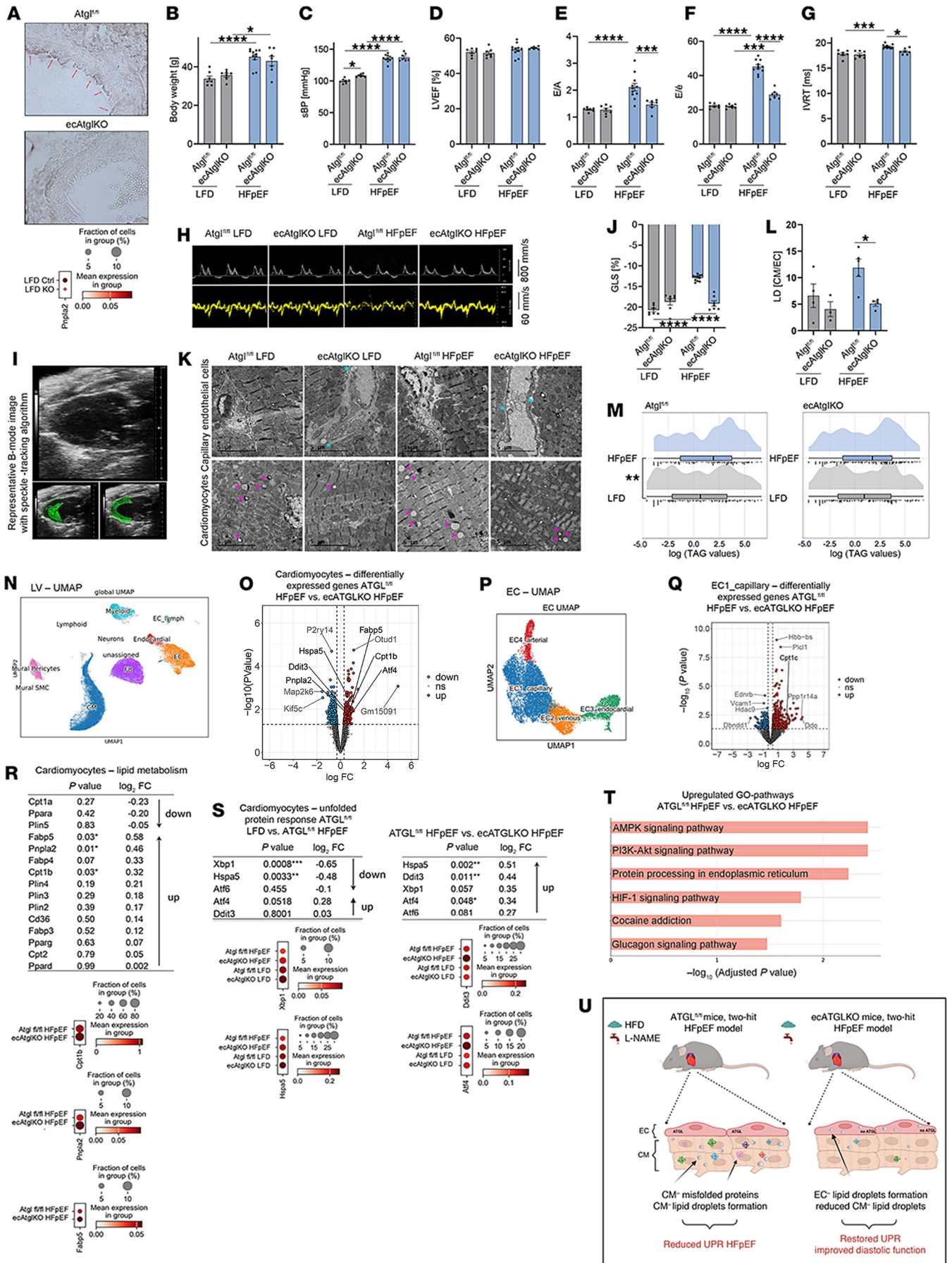


Figure 1. Endothelial deletion of ATGL protects against HFpEF. (A) Representative IHC of aortas with ATGL (brown, marked by arrows) (top). Reduced expression (single nuclei RNA-Seq, LV) of *Pnpla2* (*Atgl*) in ECs ($n = 4$; $P < 0.001$) (bottom). (B and C) Body weight (BW) and systolic blood pressure (sBP) after 15 weeks. (D–J) Echocardiographic parameters; *Atgl*^{fl/fl}-LFD ($n = 7$), *ecAtgl*KO-LFD ($n = 7$), *Atgl*^{fl/fl}-HFpEF ($n = 11$), and *ecAtgl*KO-HFpEF ($n = 7$) mice (2-way ANOVA with Bonferroni's/Tukey's multiple-comparison tests). Echocardiographic analysis of *Atgl*^{fl/fl} LFD ($n = 7$), *ecAtgl*KO LFD ($n = 7$), *Atgl*^{fl/fl} HFpEF ($n = 11$), and *ecAtgl*KO HFpEF ($n = 7$) mice (2-way ANOVA with Bonferroni's multiple comparison tests). (D) LV-ejection fraction (LVEF). (E–G) Parameters of diastolic dysfunction: E/A, E/e', IVRT. (H) Representative pulse wave (top) and tissue Doppler (bottom) images. (I) Representative B-Mode images with or without speckle-tracking algorithm. (J) Global longitudinal strain (GLS). (K) Representative transmission electron micrographs (TEM) from LVs (cyan asterisks indicate LDs in ECs; purple asterisks indicate LDs in cardiomyocytes [CM]). (L) LD quantification shown as CM/EC ratio (2-way ANOVA/Bonferroni's multiple comparison tests). (M) Triacylglycerol (TAG) content of LVs ($n = 4$) (Wilcoxon test). (N–T) Single nuclei RNA-Seq data from LV from *Atgl*^{fl/fl} and *ecAtgl*KO mice (LFD/HFpEF, $n = 4$ per group). (N) Global UMAP of all cell types present in LVs of *Atgl*^{fl/fl}-LFD/HFpEF and *ecAtgl*KO-LFD/HFpEF mice. (O) Volcano plot of differentially expressed genes (DEGs, $P < 0.05$; $\log_2FC > 0.3$). (P) UMAP of the EC cluster. (Q) Volcano plot of DEGs in capillary ECs (DEGs, $P < 0.05$; $\log_2FC > 0.3$). (R) DEGs for lipid metabolism in CM (top), significant DEGs with $P < 0.05$ as dot plots (bottom) (*Atgl*^{fl/fl}-HFpEF versus *ecAtgl*KO-HFpEF mice). (S) DEGs characteristic for UPR in CMs: *Atgl*^{fl/fl}-LFD versus *Atgl*^{fl/fl}-HFpEF (left), *Atgl*^{fl/fl}-HFpEF versus *ecAtgl*KO-HFpEF (right). (T) GO term analysis of genes upregulated in cardiomyocytes from *ecAtgl*KO-HFpEF versus *Atgl*^{fl/fl}-HFpEF mice. (U) Graphical representation of study. * $P < 0.05$, *** $P < 0.001$, **** $P < 0.0001$.

Juliane Schwanbeck,^{1,2} Max Stahnke,^{1,2} Anna Eberlein,^{1,2} Madeleine Goeritzer,^{1,2} Arndt Schulze,^{1,2} Dominique Pernitsch,³ Dagmar Kolb,³ Gernot F. Grabner,³ Theda U.P. Bartolomaeus,^{2,4,5,6} Sofia K. Forslund,^{2,4,5,6} Holger Gerhardt,^{2,5} Gabriele G. Schiattarella,^{2,5,7} Lucia Cocera Ortega,^{2,5} Natalia López-Anguita,^{2,5} Erin E. Kershaw,⁸ Henrike Maatz,^{2,5} Norbert Hübner,^{2,5,6,9} Rudolf Zechner,¹⁰ Anna Foryst-Ludwig,^{1,2} and Ulrich Kintscher^{1,2}

¹Institute of Pharmacology, Charité – Universitätsmedizin Berlin, Berlin, Germany. ²DZHK (German Centre for Cardiovascular Research), Partner Site Berlin, Germany. ³Gottfried Schatz Research Center, Medical University of Graz, Austria. ⁴Experimental and Clinical Research Center, Charité/Max Delbrück Center for Molecular Medicine (MDC), Berlin, Germany. ⁵MDC, Berlin, Germany. ⁶Charité – Universitätsmedizin Berlin, Germany. ⁷Deutsches Herzzentrum der Charité (DHZC), Berlin, Germany. ⁸Division of Endocrinology and Metabolism, Department of Medicine, University of Pittsburgh, Pennsylvania, USA. ⁹Helmholtz Institute for Translational AngioCardioScience (HI-TAC) of the MDC at Heidelberg University, Germany. ¹⁰University of Graz, Institute of Molecular Biosciences, Graz, Austria.

Address correspondence to: Ulrich Kintscher, Charité - Universitätsmedizin Berlin, Institute of Pharmacology, Hessesche Str. 3-4, 10115 Berlin, Germany. Phone: 49.30.450.525.276; Email: ulrich.kintscher@charite.de.

- Mishra S, Kass DA. Cellular and molecular pathobiology of heart failure with preserved ejection fraction. *Nat Rev Cardiol.* 2021;18(6):400–423.
- Boutagy NE, et al. Dynamic metabolism of endothelial triglycerides protects against atherosclerosis in mice. *J Clin Invest.* 2024;134(4):e170453.
- Kim B, et al. Endothelial lipid droplets suppress eNOS to link high fat consumption to blood pressure elevation. *J Clin Invest.* 2023;133(24):e173160.
- Kuo A, et al. Lipid droplet biogenesis and function in the endothelium. *Circ Res.* 2017;120(8):1289–1297.
- Sternak M, et al. Vascular ATGL-dependent lipolysis and the activation of cPLA₂-PGI₂ pathway protect against postprandial endothelial dysfunction. *Cell Mol Life Sci.* 2024;81(1):125.
- Schiattarella GG, et al. Nitrosative stress drives heart failure with preserved ejection fraction. *Nature.* 2019;568(7752):351–356.